Proceedings of the XXIII Conference on Applied Crystallography, Krynica Zdrój, Poland, September 20–24, 2015

X-Ray Diffraction Studies of the Reversible Phase Transformation in NiTi Shape Memory Alloy

Z. Lekston* and M. Zubko

Institute of Materials Science, University of Silesia, 75 Pułku Piechoty 1A, 41-500 Chorzów, Poland

In the present paper the phase transformations occurring in hot worked and heat-treated Ni-rich NiTi shape memory alloy were studied using X-ray diffraction, differential scanning calorimetry and bend and free recovery measurements. Based on conducted measurements it can be seen that in the studied alloy two-step $B2 \leftrightarrow R \leftrightarrow B19'$ phase transitions occurred. Due to the fact that during heating the phase transition $B2 \rightarrow R$ and $R \rightarrow B19'$ occurs in a very narrow temperature range and differential scanning calorimetry peaks overlap additional X-ray diffraction measurements were performed. Obtained characteristic temperatures from applied different experimental methods are in good agreement. The optimum heat-treatment was selected to obtain rods with a shape recovery temperature A_f below 37 °C to prepare prototypes of medical implants activated by patients body heat.

DOI: 10.12693/APhysPolA.130.1059

PACS/topics: 62.20.fg, 81.30.Kf, 61.05.cp

1. Introduction

It is known that near-equiatomic NiTi alloys exhibit excellent shape memory effects and superelasticity accompanied with high mechanical properties and corrosion resistance [1]. The shape memory effects are mainly attributed to the thermoelastic, reversible martensitic phase transformation. These alloys, at high temperatures, have the CsCl structure type known as the parent or austenite phase ($B2$) and at low temperatures a monoclinic structure known as the martensitic phase ($B19'$) [2]. The phase transformation course is mainly analyzed by means of differential scanning calorimetry (DSC), X-ray diffraction (XRD), transmission electron microscopy (TEM), or electrical resistivity (ER). The transformation sequence during cooling and heating can be $B2 \leftrightarrow B19'$ or $B2 \leftrightarrow R \leftrightarrow B19'$ or simply $B2 \leftrightarrow R$ under different thermal and mechanical processing techniques [3]. The R-phase (rhombohedral deformation of the $B2$ structure) appears in Ni-rich alloys after ageing or annealing at low temperatures immediately after cold working, substituting a third element and conducting thermal or thermomechanical cycling [4, 5]. Ageing of Ni-rich NiTi alloys leads to the progressive precipitation of Ni_4Ti_3, Ni_3Ti_2 and Ni_3Ti precipitates. The amount of precipitates is proportional to the increase of ageing time, temperature, and Ni content [6, 7]. Ni_4Ti_3 precipitates are coherent with the matrix and mostly influence the course of the transformation and mechanical properties of the alloys. Usually, a one-stage transformation $B2 \leftrightarrow B19'$ occurs in solution treated Ni-rich NiTi alloys and a two-stage transformation $B2 \leftrightarrow R \leftrightarrow B19'$ occurs after additional ageing treatment [8]. The $B2 \leftrightarrow B19'$ and the $R \leftrightarrow B19'$ transformation are characterized by large lattice distortion and large transformation hysteresis. In contrast, the $B2 \leftrightarrow R$ transformation reveals by a small lattice distortion and a small temperature hysteresis [9]. All three transformations involve lattice distortions and possess martensitic nature. The presence of the Ni_4Ti_3 particles favours the formation of R-phase and produces a strong resistance to the formation of the $B19'$ martensite. Therefore transformations during cooling occur in two steps $B2 \rightarrow R \rightarrow B19'$. In the recent literature a tree-stage or multistage martensitic transformation in aged Ni-rich NiTi alloys were reported [10–13]. Generally, the occurrence of the multiple stage transformations is attributed to precipitation-induced inhomogeneity of the matrix, both in terms of composition and internal stress fields. The transformations during cooling and heating are characterized by M_s and M_f which are the initial and final temperatures of the martensite transformation whereas A_s and A_f are the initial and finish temperatures of the austenite transformation, respectively. The transformation behaviour of the R-phase is defined by four characteristic temperatures, R_{cs}, R_{cf} and R_{hs}, R_{hf} which are the start and finish temperatures of the R-phase transformation recorded during cooling and heating, respectively. The R-phase transformation can be easily observed during temperature X-ray diffraction measurements, when during cooling the splitting of $(110)_{B2}$ and $(211)_{B2}$ diffraction reflections takes place [14–19]. All the transformations are sensitive to variations in metallurgical conditions as well as chemical composition and heat and thermo-mechanical treatments. The courses of phase transformations after different heat treatment and the characteristic temperatures of the phase transformations in semi-finished NiTi products is important from the view of practical applications.

In this work the phase transformations occurring in heat-treated NiTi shape memory alloy was studied using XRD, DSC, and bend and free recovery (BFR) measurements done during heating.

2. Material and methods

In the present study the vacuum induction melted Ti–50.8 at.% Ni-alloy was used. Melting and casting of the

*corresponding author; e-mail: zdzislaw.lekston@us.edu.pl

NiTi alloy was carried out in the Balzers VSG 10 vacuum induction furnace in the Research and Development Laboratory for Aerospace Materials, at the Rzeszów University of Technology. The ingot with its weight of 900 g (Fig. 1) was homogenized in the electrical vacuum furnace at 900 °C for 48 h in the vacuum of 2×10^{-5} Pa.

Fig. 1. A view of ingot of studied NiTi alloy.

The rods from ingot were obtained by hot-smith forging and hot forging in swaging machine to diameter of approximately 3 mm. The samples with 70 mm long and 3.2 mm in diameter were quenched from 800 °C/15 min and subsequently aged at the 400, 450, and 500 °C during 30 and 60 min, respectively. The course of phase transitions and its characteristic temperatures were determined from DSC measurement for samples after each heat treatment. The measurements were carried out on DSC 1 Mettler Toledo in the temperature range from –120 °C to +120 °C with 10 °C/min heating and cooling rate. The X-ray powder diffraction (XRD) measurements were performed over 2θ range from 37° to 47° on a PANalytical Empyrean diffractometer. Measurements were performed at temperatures from –180 to 250 °C using Anton Paar TTK450 Low-Temperature chamber equipped to the diffractometer. The measurements performed with 5 °C steps resulted in heating rate of 0.7 °C/min. Shape recovery studies were carried out using three-point bending and free recovery (BFR) ASTM F2082-06 tests with heating rate of 10 °C/min.

3. Results and discussion

3.1. Differential scanning calorimetry

Figure 2 shows the DSC thermograms recorded at the cooling and heating cycle for samples after solution treatment at 800 °C for 15 min and for samples after ageing at 400, 450, and 500 °C for 30 and 60 min. In the sample after solution treatment (800 °C/15 min) only one step transformation takes place.

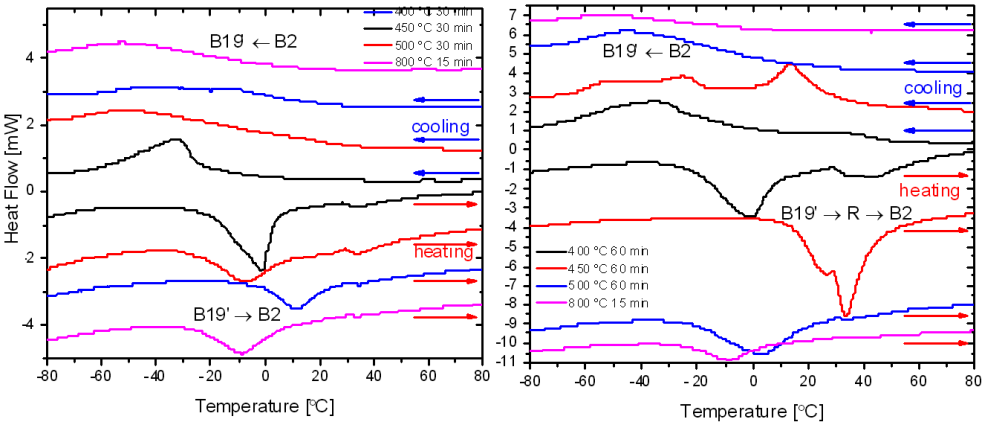

Fig. 2. Comparison of DSC cooling/heating curves for Ti–50.8 at.% Ni after solution treatment at 800 °C for 15 min and after ageing at 400, 450, and 500 °C for 30 min (left) and for 60 min (right).

On cooling and heating the transition between parent phase and martensite phase transformation ($B2 \leftrightarrow B19'$) is observed. In the sample after solution treatment the martensitic transformation during the cooling takes place in the temperature range of –30 to –70 °C and on heating the reverse transformation occurs in the range of –30 to 10 °C. Ageing at temperatures of 450 and 500 °C for 30 min resulted in slight increase of the characteristic temperatures of phase transformations. The DSC curves recorded during the cooling and heating for the aged samples reveal double thermal effects as an evidence of a two-stage course of transformation $B2 \leftrightarrow R \leftrightarrow B19'$. The two-stage nature of the transformations were also observed on the DSC curves of samples aged at 400 and 500 °C during 60 min (Fig. 2). On the DSC curve recorded during cooling for a sample of aged at 450 °C for 60 min there are three exothermic peaks in the temperature range of about +25 to +5 °C, –25 to –35 °C and –45 to –70 °C. The first peak is associated to the phase transformation occurring from $B2$ parent phase to the R phase ($B2 \rightarrow R$), the second peak with the transformation of rhombohedral R phase to martensitic phase ($R \rightarrow B19'$), in region of the grain boundary (affected by heterogeneous precipitation of Ni_4Ti_3), while the third peak is associated with the phase transformation of the R phase to the martensitic phase ($R \rightarrow B19'$) in the grain interior [20]. During heating the phase transformations in the sample takes place at the sequence of $B19' \leftrightarrow R \leftrightarrow B2$. The increase of the phase transformation temperature range observed on DSC curves for

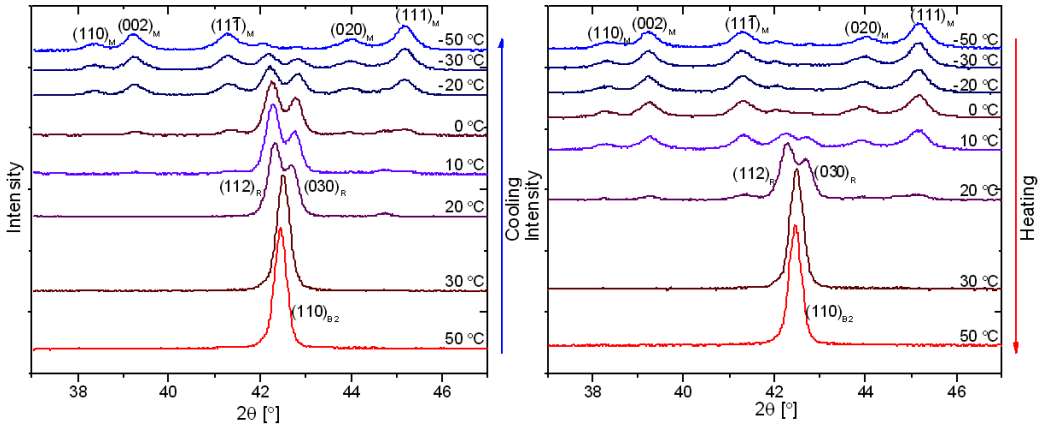

Fig. 3. X-ray diffraction patterns recorded during cooling (left) and heating (right) of the sample after solution treatment and ageing at 500 °C for 60 min.

samples after ageing, in comparison to solution treated samples can be explained by the reduction of nickel content in the alloy matrix as a result of the Ni_4Ti_3 phase formation enriched in nickel during precipitation process [6, 13, 20]. To confirm the occurrence of the R phase during phase transition the X-ray studies were carried out during the cooling and heating of selected samples after ageing. Diffraction patterns recorded for the sample solution treated at (800 °C/15 min) and then aged at 500 °C for 60 min are shown in Fig. 3.

3.2. X-ray diffraction study of the reversible transformations

X-ray powder diffraction patterns, shown in Fig. 3, indicate the courses of phase transitions in the studied NiTi alloy. On the diffraction pattern recorded at 20 °C splitting of the peak 110_{B2} into characteristic doublet $(112)_R$ and $(030)_R$ of the R phase is visible. During cooling at the temperature of 10 °C the very weak diffraction lines $(110)_M$, $(002)_M$, $(11\bar{1})_M$, $(020)_M$ and $(111)_M$ appeared indicating the start of the martensitic transformation. Upon further cooling there are visible decrease of the intensity of the R phase doublet and increase of the martensitic diffraction lines.

Thus, during cooling the phase transformation occurs in two stages with a sequence: $B2 \rightarrow R$ and $R \rightarrow B19'$. During heating in the sample after ageing at 500 °C/60 min changes also take place with the participation of the R phase by the sequence of $B19' \rightarrow R \rightarrow B2$. Due to the fact that during heating the phase transition $B2 \rightarrow R$ and $R \rightarrow B19'$ occur in very narrow temperature range and DSC peaks overlap (Fig. 2). The observed diffraction $(110)_{B2}$ peaks were deconvoluted by fitting pseudo-Voigt functions to the experimental data, to confirm the changes during cooling and heating occur with the participation of the R phase.

3.3. The study of one-shape memory effect by bend and free recovery ASTM test

The one-way shape recovery effect of studied samples was observed after bending the sample at temperature below –70 °C and during free recovery measurements in heating cycle. Normalized shape recovery vs. temperature curves for samples after different heat treatments are shown in Fig. 4. The characteristic temperatures for reversible phase transitions have been shifted to the higher values after ageing both for 30 and 60 min.

On the shape recovery curves of samples after ageing at 400 and 450 °C there is visible a bending in a temperature range of approximately 30 to 40 °C which is an evidence of two-stage phase transformation during heating. The shape recovery of the samples aged at 500 °C for 30 and 60 min occurs in a single stage within a desired narrow temperature range below 37 °C (blue curves in Fig. 4).

4. Conclusions

The obtained results from investigations of Ni-rich Ti–50.8 at.% Ni alloy by using DSC, XRD, and BFR techniques can be summarized as follows. A one-stage, reversible transformations $B2 \leftrightarrow B19'$ in the samples after solution treatment occur. In the samples after ageing two-stage $B2 \leftrightarrow R \leftrightarrow B19'$ phase transitions were observed. From X-ray diffraction investigations of phase transformations of samples aged at 500 °C it is visible that on cooling, two well separated peaks appear corresponding to the two transformations: austenite to the R phase ($B2 \rightarrow R$) and the R phase to martensite ($R \rightarrow B19'$), respectively. During heating the phase transitions occur with a intermediate R phase according to a sequence ($B19' \rightarrow R$) and then ($R \rightarrow B2$). During heating the transitions temperatures of sample solution treated at 800 °C and aged at 500 °C are in desired temperature range below the patient body temperature. Rods after ageing at 500 °C for 30 and 60 min recover the shape at the desired temperature below 37 °C and are suitable for the preparation of orthopaedic staples operating under the influence of body heat of the patient. For the preparation of the staples to the fixation of bone fractures working under the influence of patients' body heat rods after ageing at 500 °C for 30 min have been selected.

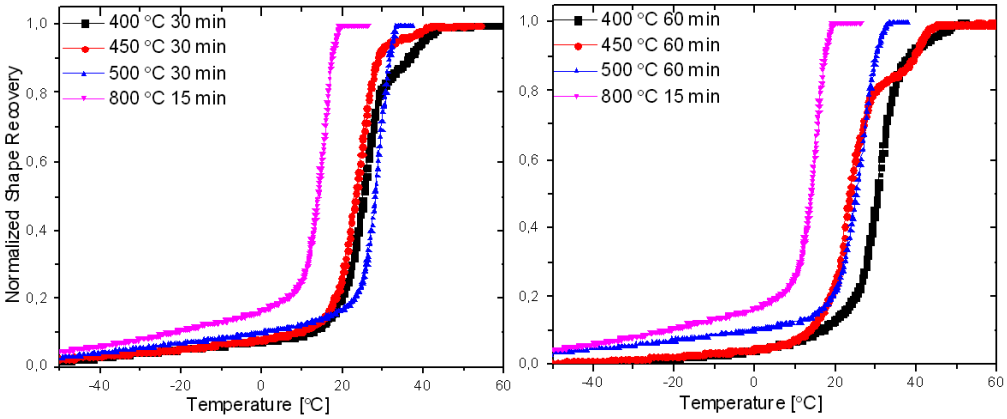

Fig. 4. The curves of shape recovery vs. temperature measured for samples after solution treatment and after ageing at temperatures 400, 450, and 500 °C for 30 min (left) and 60 min (right).

Acknowledgments

The study uses the results of the research funded by the National Centre for Research and Development under the project No. INNOTECH-K1/IN1/46/157239/NCBR/12.

References

[1] T. Yoneyama, S. Miyazaki, *Shape Memory Alloys for Biomedical Applications*, Woodhead Publ., Cambridge 2009.

[2] K. Otsuka, X. Ren, *Prog. Mater. Sci.* **50**, 511 (2005).

[3] Y. Liu, H. Yang, A. Voigt, *Mater. Sci. Eng. A* **360**, 350 (2003).

[4] T. Goryczka, H. Morawiec, *J. Alloys Comp.* **367**, 137 (2004).

[5] T. Goryczka, H. Morawiec, *J. Phys. IV, (France)* **112**, 693 (2003).

[6] R.R. Adharapurapu, F. Jiang, K.S. Vecchio, *Mater. Sci. Eng. A* **527**, 1665 (2010).

[7] Y. Zheng, F. Jiang, L. Li, H. Yang, Y. Liu, *Acta Mater.* **56**, 736 (2008).

[8] O. Bojda, G. Eggeler, A. Dlouhy, *Scr. Mater.* **53**, 99 (2005).

[9] J.I. Kim, Y. Liu, S. Miyazaki, *Acta Mater.* **52**, 487 (2004).

[10] J. Khalil-Allafi, X. Ren, G. Eggeler, *Acta Mater.* **50**, 793 (2002).

[11] J. Khalil-Allafi, A. Dlouhy, G. Eggeler, *Acta Mater.* **53**, 3971 (2005).

[12] Y. Zhou, J. Zhang, G. Fan, X. Ding, J. Sun, X. Ren, K. Otsuka, *Acta Mater.* **53**, 5365 (2005).

[13] G. Fan, W. Chen, S. Yang, J. Zhu, X. Ren, K. Otsuka, *Acta Mater.* **52**, 4351 (2004).

[14] H.C. Ling, R. Kaplow, *Metall. Trans.* **11A**, 77 (1980).

[15] J. Uchil, F.M. Braz Fernandez, K.K. Mahesh, *Mater. Character.* **58**, 243 (2007).

[16] M. Pattabi, K. Ramakrishna, K.K. Mahesh, *Mater. Sci. Eng. A* **448**, 33 (2007).

[17] Z. Lekston, E. Łągiewka, *Archiv. Mater. Sci. Eng.* **28**, 665 (2007).

[18] Z. Lekston, M. Zubko, *Solid State Phenom.* **203-204**, 125 (2013).

[19] Z. Lekston, M. Zubko, K. Prusik, D. Stróż, *J. Mater. Eng. Perf.* **23**, 2362 (2014).

[20] Y. Zhang, Z. Jiang, Y. Zhao, M. Tang, *Trans. Nonferrous Met. Soc. China* **22**, 2685 (2012).